

Forsmark site investigation

Interpretation of petrophysical data from the cored boreholes KFM04A, KFM05A and KFM06A

Håkan Mattsson, Hans Thunehed, Hans Isaksson
GeoVista AB

August 2005

Svensk Kärnbränslehantering AB

Swedish Nuclear Fuel
and Waste Management Co
Box 5864
SE-102 40 Stockholm Sweden
Tel 08-459 84 00
+46 8 459 84 00
Fax 08-661 57 19
+46 8 661 57 19



Forsmark site investigation

Interpretation of petrophysical data from the cored boreholes KFM04A, KFM05A and KFM06A

Håkan Mattsson, Hans Thunehed, Hans Isaksson
GeoVista AB

August 2005

Keywords: Petrophysics, Anisotropy, Magnetic susceptibility, AMS, Density, Porosity, Resistivity, Induced polarisation, Gamma-ray spectrometry, Forsmark, AP PF 400-05-031.

This report concerns a study which was conducted for SKB. The conclusions and viewpoints presented in the report are those of the authors and do not necessarily coincide with those of the client.

A pdf version of this document can be downloaded from www.skb.se

Abstract

This report presents the compilation and interpretations of petrophysical measurements on 15 rock samples from the cored boreholes KFM04A, KFM05A and KFM06A. The purpose of petrophysical measurements is to gain knowledge of the physical properties of different rock types. The information is used, for example, to support geophysical measurements and to support the geological bedrock mapping.

The results from these investigations show that there is a general agreement between the geological rock classification and the geophysical rock classification indicated by the density-susceptibility diagrams. A significant deviation from this is the metagranodiorite (B7) sample from KFM04A, which plots as a low density granite. A very high Q-value (12.5) is reported for a metagranite to granodiorite sample in KFM06A. The result indicates that the magnetic mineralogy of the rock sample deviates from what is normal for this rock type group. Apart from this deviation, the Q-values are moderate or low in all three boreholes.

The AMS data indicate that the rocks in the vicinities of the three investigated boreholes have suffered from different types of deformation. The samples of KFM04A have flattened ellipsoids and partly strong degree of anisotropy, which indicates strong compressive deformation. In KFM05A the AMS fabric is poorly developed, which is characteristic for a low degree of deformation. The rock samples in KFM06A show elongated AMS ellipsoids, which probably indicate a dominant stretching type of deformation.

All investigated rock samples show fairly normal porosity values for crystalline rocks. The KFM04A samples have electrical properties indicative of strong surface conductivity that probably is related to presence of fine-grained phyllo-silicates like e.g. chlorite. One sample from KFM04A containing sulphides has low resistivity and high induced polarisation effect.

The sampled rock types in all three boreholes in general show a normal distribution of potassium, uranium and thorium. However, in the deeper part of KFM06A both aplitic metagranite and metagranite-granodiorite show a strong depletion in potassium, with a content of 0.2–0.6% K.

Sammanfattning

Föreliggande rapport presenterar en sammanställning och tolkning av petrofysiska mätningar på 15 borrhärneprover från KFM04A, KFM05A och KFM06A. Syftet med de petrofysiska mätningarna är att bestämma fysikaliska egenskaper hos olika bergarter. Informationen används bl a som stödande data vid tolkning av geofysiska mätningar och bergartskarteringen.

Resultaten från undersökningarna visar en generell överensstämmelse mellan den geologiska bergartsklassificeringen och den klassificering som görs med hjälp av densitet-susceptibilitetsdiagram. En avvikelse utgörs av ett metagranodioritprov i KFM04A som i densitet-susceptibilitetsdiagrammet klassas som en granit med låg densitet. I KFM06A har det uppmätts ett mycket högt Q-värde (12,5) för en metagranit till granodiorit. Bortsett från denna avvikelse är Q-värdena på övriga prover låga eller normala.

AMS-data indikerar att berget i närheten av de undersökta borrhålen har utsatts för varierande typ av deformation. Prover från KFM04A uppvisar tillplattade anisotropi-ellipsoider och bitvis hög grad av anisotropi, vilket tyder på kraftig deformation som dominerats av tryck. I KFM05A är anisotropiellipsoiderna nästan neutrala (klotformade) och graden av anisotropi är låg till moderat, vilket tyder på låg grad av deformation. Proverna i KFM06A har utsträckta ellipsoider, vilket troligen indikerar en deformation dominerad av dragspänning.

Alla undersökta prover har porositetsvärden som är normala för kristallint berg. Proverna i KFM04A har elektriska egenskaper som är typiska för kraftig ytkonduktivitet, vilket sannolikt kan kopplas till förekomst av finkorniga phyllosilikater, t ex klorit. Ett prov från KFM04A innehåller sulfider och har låg resistivitet och hög inducerad polarisation.

Gammaspektrometermätningarna visar att alla undersökta prover generellt har en normal fördelning av kalium, uran och thorium. Längs de djupare delarna av KFM06A visar dock både aplitisk metagranit och metagranit till granodiorit på en kraftig utarmning av kalium, med halter kring 0,2–0,6 % K.

Contents

1	Introduction	7
2	Objective and scope	9
3	Equipment	11
3.1	Description of software for analyses of petrophysical data	11
4	Execution	13
4.1	Sample handling and geological coding	13
4.1.1	Petrophysical samples	13
4.1.2	Gamma ray spectrometry	14
4.1.3	Sample selection and coding	14
4.2	Analyses and processing	15
4.2.1	Density and magnetic properties	15
4.2.2	Anisotropy of magnetic susceptibility (AMS)	16
4.2.3	Electrical properties	16
4.2.4	Gamma ray spectrometry	17
4.3	Nonconformities	18
5	Results	19
5.1	Density and magnetic properties	19
5.1.1	KFM04A	19
5.1.2	KFM05A	20
5.1.3	KFM06A	21
5.2	Anisotropy of magnetic susceptibility (AMS)	22
5.2.1	KFM04A	22
5.2.2	KFM05A	22
5.2.3	KFM06A	23
5.3	Electrical properties and porosity	24
5.3.1	KFM04A	24
5.3.2	KFM05A	25
5.3.3	KFM06A	26
5.4	Gamma ray spectrometry	27
5.4.1	KFM04A	27
5.4.2	KFM05A	28
5.4.3	KFM06A	28
6	Compilation of petrophysical parameters	33
6.1	Comments on the results	34
	References	37
	Appendix 1	39

1 Introduction

SKB performs site investigations for localization of a deep repository for high level radioactive waste. The site investigations are performed at two sites, Forsmark and Oskarshamn. This document reports the results gained from the interpretation of petrophysical measurements on samples from the cored boreholes KFM04A, KFM05A and KFM06A in Forsmark (Figure 1-1).

The petrophysical determinations include magnetic susceptibility, remanent magnetization, anisotropy of magnetic susceptibility (AMS), density, porosity, electric resistivity, induced polarization and gamma-ray spectrometry. The gamma-ray spectrometry measurements were performed by the Geological Survey of Sweden, whereas the other parameters were measured by the Petrophysical Laboratory at the Division of Applied Geophysics, Luleå University of Technology.

The interpretation presented in this report is performed by GeoVista AB in accordance with the instructions and guidelines from SKB (activity plan AP PF 400-05-031 and method descriptions SKB MD 132.001 and SKB MD 230.001, SKB internal controlling documents). The controlling documents are listed in Table 1-1.

No field work has been performed.

Table 1-1. Controlling documents for the performance of the activity.

Activity plan	Number	Version
	AP PF 400-05-031	1.0
Method descriptions	Number	Version
Metodbeskrivning för bestämning av densiteten och porositeten hos det intakta berget.	SKB MD 132.001	1.0
Metodbeskrivning för mätning i laboratorium av bergarters petrofysiska egenskaper.	SKB MD 230.001	1.0

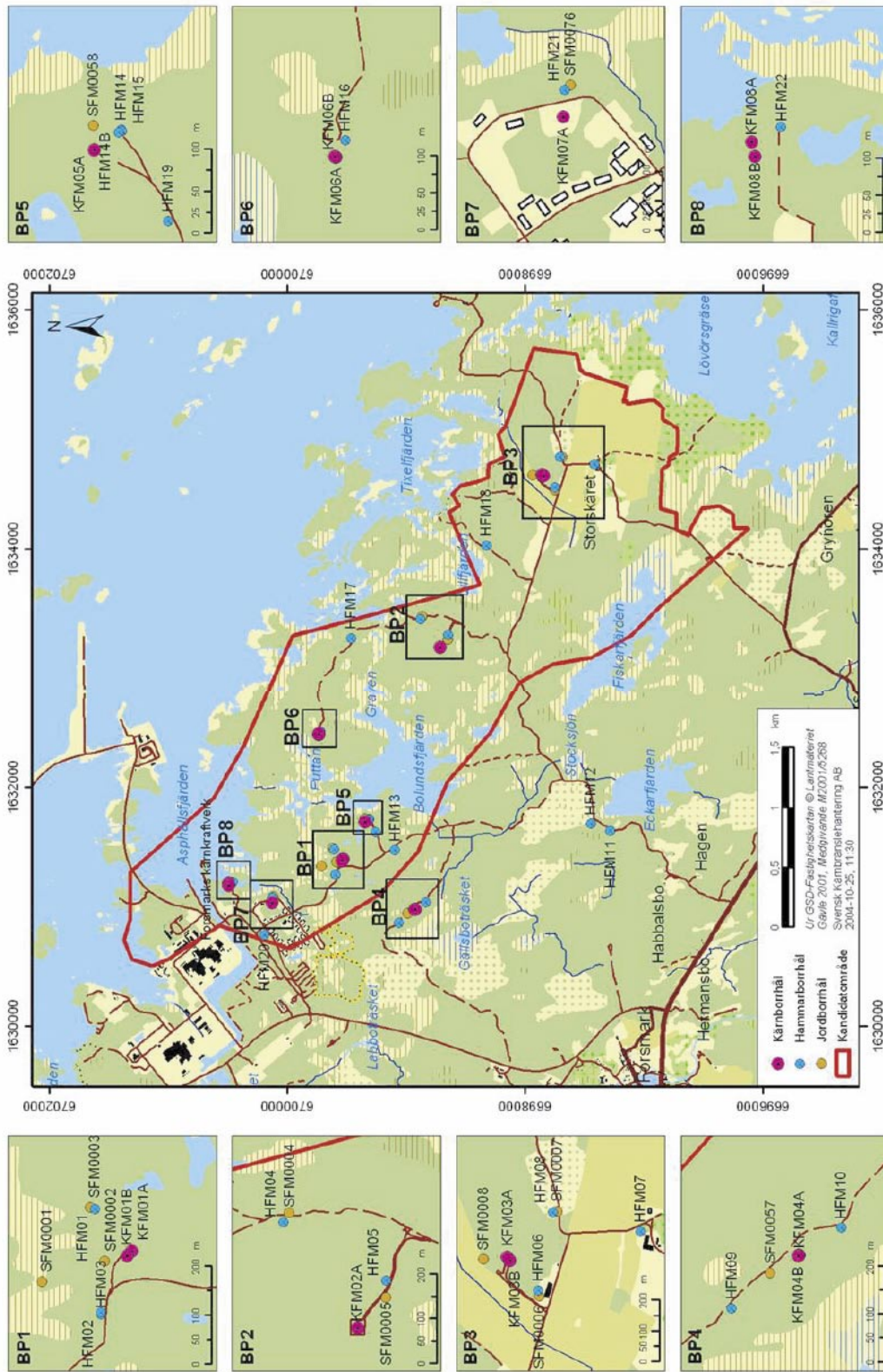


Figure 1-1. Map showing the location of the investigated boreholes; KFM04A, KFM05A and KFM06A.

2 Objective and scope

The purpose of petrophysical measurements is to gain knowledge of the physical properties of different rock types. This information is used to increase the understanding of geophysical logging measurements, to perform quality controls of the logging data and to support the geological core mapping. Rock fabric information and parameters related to grain size are also achieved from the petrophysical measurements.

The work comprises statistical processing and evaluation of results from measurements on core samples. The analyses were made with respect to rock type characteristics and the distribution with depth of the measured properties.

3 Equipment

3.1 Description of software for analyses of petrophysical data

The software used for the processing and interpretation are Grapher (Golden Software), Microsoft Excel, Anisoft (AGICO Inc).

4 Execution

4.1 Sample handling and geological coding

The sampling for gamma-ray spectrometry analysis was performed separately from the sampling of the other petrophysical parameters. The handling and coding of the petrophysical samples is described in paragraph 4.1.1 and the handling of the gamma-ray spectrometry samples in paragraph 4.1.2. Sample selection and geological coding is described in paragraph 4.1.3.

4.1.1 Petrophysical samples

Each petrophysical sample is a c 200 mm long split core with a diameter of c 50 mm. The samples were assigned an identity code comprising “Borehole identity”, “section up” and “section low”. The electrical measurements were performed on the split cores samples. Four 22 mm long specimens were then drilled from each of the original core samples, perpendicular to the core axis. Each specimen was given a specimen number, to separate them from each other. The magnetic measurements were performed on single specimens. All specimens plus, if possible, the remains of the core sample, were then assembled and the density (wet and dry) and porosity measurements were performed. A scheme showing the number and type of determinations per sample, for each borehole respectively, is presented in Table 4-1 below. Measurement techniques and sample handling are described in more detail in /1/.

The samples are not oriented with reference to any co-ordinate system, there is only a mark indicating section up and section low. The orientation of the remanence vectors and the principal anisotropy axes are therefore only made with reference to the core axis. Declination data of these parameters are consequently meaningless but inclination variations may be possible to interpret if the borehole is sub-vertical. However, the dip of KFM04A is c 44–61°, KFM05A has a dip of 53–63° and KFM06A dips c 51–60°. The shallow dip of the three boreholes makes the interpretation of the inclination data meaningless; for example, the uncertainty of an inclination data reading of a sample from KFM04A could be as much as $\pm 46^\circ$.

Table 4-1. Number and type of petrophysical determinations on each core sample from KFM04A, KFM05A and KFM06A.

Borehole	Number of samples	Density/ Porosity	AMS	Remanence	Resistivity/IP
KFM04A	5	1	4	1	1
KFM05A	5	1	4	1	1
KFM06A	5	1	4	1	1

4.1.2 Gamma ray spectrometry

Gamma-ray spectrometry was carried out on samples taken for geochemical analyses. The handling of these samples is described in /2/ and includes grinding. The spectrometry measurements were carried out on this grinded material.

From each sample, two 60 g fractions (sub-samples) were extracted and put into plastic pots, which were hermetically sealed and stored for three weeks awaiting isotope equilibrium.

The samples were given ID:s according to SKB standards (borehole ID, sec up, sec low), the same ID:s as the corresponding geochemical samples. In addition, the samples were assigned a unique SGU-ID in order to separate the sub-samples. Geological coding of the samples was made as part of the work presented in /2/.

Measurements were made of each sub-sample according to the routines developed at the petrophysical laboratory of SGU. The measuring time was one hour and several samples were measured two, and in some cases three times for the purpose of reproducibility control. Background radiation was checked daily and after the measuring of every 10–15 samples, K, U and Th standards were measured.

4.1.3 Sample selection and coding

The selection of sampling (measurement) locations was performed in co-operation with the responsible geologist. Each petrophysical sample was collected in the direct vicinity of geological samples taken for thin section analyses, geochemical analyses and gamma-ray spectrometry analyses. This allows reliable comparisons between petrophysical, gamma-ray spectrometric and geological data. The geological characteristics of the investigated rocks are presented in /3/.

An established geological coding system was used containing four major rock groups (A, B, C and D) and sub-groups of rock types for each rock group respectively. Each rock sample was classified according to this system, Table 4-2.

The core samples collected for the petrophysical and gamma-ray spectrometry analyses include (exact co-ordinate along the drill core is presented in Tables 6-1, 6-2 and 6-3):

KFM04A

1 metagranodiorite sample (B7; section length c 116–117 m), 2 metagranite-granodiorite samples (B8; section lengths c 186–187 m and 271 m), 1 amphibolite sample (B4; section length c 737 m) and 1 intermediate metavolcanite sample (A1, section length c 124–125 m). All samples have suffered from strong plastic deformation.

KFM05A

3 metagranite-granodiorite samples (B8; section lengths c 152 m, 272 m and 298–299 m), 1 amphibolite sample (B4; section length c 356 m) and 1 metagranitoid, (group C sample; section length c 691 m).

Table 4-2. Code table for the different rock groups.

Rock Group (SGU)	Code (SKB)	Composition (and grain size)
		Name (IUGS/SGU)
A1	103076	Dacite and andesite, metamorphic
A1	106000	Sedimentary rock, metamorphic
A2	109014	Magnetite mineralization associated with calc-silicate rocks
A3		Veined gneiss
A4	108019	Calc-silicate rock (skarn)
A5	109010	Pyrite-pyrrhotite-chalcopyrite-sphalerite mineralisation
B1	101004	Ultramafic rock (olivine-hornblende pyroxenite)
B2/B3	101033	Diorite, quartz diorite and gabbro, metamorphic
B4	102017	Amphibolite
B5/B6	101054	Tonalite and granodiorite, metamorphic
B7	101056	Granodiorite, metamorphic
B8/B9	101057	Granite and granodiorite, metamorphic, medium-grained (the most common rock type in the candidate area)
B10	101058	Granite, metamorphic, aplitic
	111051	Granitoid, metamorphic
C	101051	Granodiorite, tonalite and granite, metamorphic, fine- to medium-grained
D1	111058	Granite, fine- to medium-grained
D2/D3	101061	Pegmatitic granite, pegmatite

KFM06A

4 aplitic metagranite samples (B10; section lengths c 636 m, 818 m, 850–851 m and 937–938 m) and 1 metagranite-granodiorite sample (B8, section length c 757 m). The samples collected at 818 m, 850–851 m, 937–938 and 757 m have suffered from strong alteration.

4.2 Analyses and processing**4.2.1 Density and magnetic properties**

In order to get a better picture of the data and to increase the possibility to compare different data sets and data from different rock types, some sub-parameters are often calculated from the density, the magnetic susceptibility and the magnetic remanence. Two such sub-parameters are the silicate density and the Q-value (Königsberger ratio). The silicate density /4/ provides an estimation of the rock composition and is calculated by correcting the measured total density for the content of ferromagnetic minerals (e.g. magnetite and pyrrhotite) by use of the magnetic susceptibility. The Q-value /5/ is the quotient between the remanent and induced magnetization. The Q-value thus indicates the contribution of the remanent magnetization to the measured anomalous magnetic flux density and is therefore an important parameter when interpreting and modelling ground and airborne magnetic data. The Q-value is also grain size dependent and indicates what ferromagnetic minerals that is present in the rock.

In this investigation the so called density-susceptibility rock classification diagrams were used. The y-axis in these diagrams displays the magnetic susceptibility on the left hand side and the estimated magnetite content to the right. It has been shown that in rocks in which the magnetic susceptibility is primarily governed by magnetite, there is a fairly good correlation between the magnetic susceptibility and the magnetite content /6/. However, the scatter is fairly high so predictions of the volume-percent magnetite in rocks based on the magnetic susceptibility should be used with caution. The x-axis displays the wet density. The silicate density curves are based on equations from Henkel 1991 /4/, and the average densities of each rock type originate from Puranen 1989 /7/. The diagram should be read in the way that if a rock sample plots on, or close to, a “rock type curve” it is indicated that the rock should be classified according to the composition of this rock type. Since there is often a partial overlap of the density distributions of different rock types, there is always a certain degree of uncertainty in the classification. A sample plotting in between, for example, the granite and granodiorite curves should thus be classified as granite to granodiorite.

4.2.2 Anisotropy of magnetic susceptibility (AMS)

The four measurements on individual specimens allow a calculation of mean directions of the principal AMS axes (called the site mean direction) and corresponding “site mean value” of the degree of anisotropy (P), degree of lineation (L), degree of foliation (F) and ellipsoid shape (T). When calculating the site mean values of the P, L, F and T parameters, the orientations of the ellipsoids of each specimen are taken into account. Vector addition is applied to the three susceptibility axes of the four specimens from the site, which results in a “site mean ellipsoid”. The site mean values of the anisotropy parameters thus give information of the site as a whole and are not just “simple” average values. According to statistical demands at least six measurements (specimens) are required for estimating uncertainty regions of the calculated mean directions. No such calculations were therefore performed. Instead, the data quality of each site was evaluated by visual inspection and site mean directions based on scattered specimen directions were rejected. For further descriptions of the method please see e.g. /8/ or /9/.

4.2.3 Electrical properties

The contrast in resistivity (ρ) between silicate minerals and more conducting media like water or sulphides/graphite is extremely high. The bulk resistivity of a rock is therefore more or less independent of the type of silicate minerals that it contains. Electric conduction will be almost purely electrolytic if the rock is not mineralised. Archie’s law /10/ is frequently used to calculate the conductivity ($1/\rho$) of sedimentary rocks.

$$\sigma = a \cdot \sigma_w \cdot \varphi^m \cdot s^n$$

where

σ = bulk conductivity (=1/ ρ , S/m)

σ_w = pore water conductivity (S/m)

φ = volume fraction of pore space

s = fraction of pore space that is water saturated

a, m, n = dimensionless numbers, $m \approx 1.5$ to 2.2

Archie's law has proved to work well for rocks with a porosity of a few percent or more. Old crystalline rocks usually have a porosity of 0.1 to 2% and sometimes even less. With such low porosity the interaction between the electrolyte and the solid minerals becomes relevant. Some solids, especially clay minerals, have a capacity to adsorb ions and retain them in an exchangeable state /11/. This property makes clays electrically conductive but the same property can to some degree be found for most minerals. The resulting effect, surface conductivity, can be accounted for by the parameter a in Archie's law. The relative effect of surface conductivity will be greatly reduced if the pore water is salt. The amount of surface conductivity is dependent upon the grain size and texture of the rock. Fine grained and/or mica- or chlorite-rich, foliated rocks are expected to have a large relative portion of thin membrane pore spaces that contribute to surface conductivity.

The electric resistivity is in reality not a simple scalar. Most rocks show electric anisotropy and the resistivity is thus a tensor. On a micro-scale the anisotropy is caused by a preferred direction of pore spaces and micro fractures.

The induced polarisation effect (IP) can be caused by different mechanisms of which two are the most important. When the electric current passes through an interface between electronic and electrolytic conduction there is an accumulation of charges at the interface due to the kinetics of the electrochemical processes involved. Such situations will occur at the surface of sulphide, oxide or graphite grains in a rock matrix with water filled pores. The second mechanism is related to electric conduction through thin membrane pore spaces. In this case an accumulation of charges will occur at the beginning and end of the membrane. The membrane polarisation is thus closely related to the surface conduction effect mentioned above for electric resistivity. Fine grained and/or mica- or chlorite-rich, foliated rocks are therefore expected to show membrane polarisation. Also, the effect of membrane polarisation is greatly reduced in salt water in the same way as surface conductivity.

A correction for drift caused by drying of the sample during measurements is done automatically by the instrumentation software by comparing the harmonics of low frequency measurements with the base frequency result of the next higher frequency.

The resistivity data were compared with the measured porosity in order to make a fit in accordance to Archie's law.

Apparent values of m in Archie's law can be estimated from measurements of resistivity in salt water since the relative effect of surface conductivity becomes small there. High values will be indicative for samples with a large portion of vugs, constrictions and crooked pore paths. Low values will indicate fairly straight pore paths with small variations in cross-sectional area. Using the known values of σ , σ_w and ϕ , an apparent value of the parameter a was calculated for measurements in fresh water. High values will correspond to a large contribution from surface conductivity and vice versa.

4.2.4 Gamma ray spectrometry

The gamma ray spectrometry method is based on the naturally occurring radioactive isotopes of potassium, uranium and thorium, and gives information on the content of these elements. The data is useful for bedrock and soil mapping as well as radon investigations.

The data processing has included calculation of e.g. mean values, errors, gamma index and natural exposure rate for each sub-sample and, based on these results, for the main samples;

The gamma index have been calculated according to SIG standards as

$$C_K/3,000 + C_U/300 + C_{Th}/200$$

where C is the concentration of the elements in Becquerel/kg.

The natural exposure rate ($\mu\text{R/h}$) has been calculated according to /12/ as

$$1.505 \times K [\%] + 0.625 \times U [\text{ppm}] + 0.310 \times Th [\text{ppm}]$$

The results of the gamma-ray spectrometry laboratory measurements and data processing are presented in Appendix 1 and further analyzed in paragraph 5.4.

4.3 Nonconformities

No nonconformities are reported.

5 Results

5.1 Density and magnetic properties

5.1.1 KFM04A

The two metagranite to metagranodiorite samples have fairly low density (c 2,650 kg/m³), which corresponds to granite rock (Figure 5-1). The single metagranodiorite sample has even lower density, and from a petrophysical point of view the rock could almost be classified as leucocratic granite. The amphibolite has a characteristic signature with low magnetic susceptibility and high density (2,907 kg/m³) and the intermediate metavolcanic rock sample plots between the granodiorite (rhyo-dacite) and tonalite (dacite) classification curves.

The Q-values of all five samples from KFM04A are low (Figure 5-2), ranging from 0.02 to 0.14, which is an indication that the remanent magnetization has little influence on the total magnetic field. The fairly large variation in magnetic susceptibility between the two metagranite to metagranodiorite samples is not reflected in the Q-values, and this is a clear indication that the variation solely depends on variations in magnetite content between the two rocks.

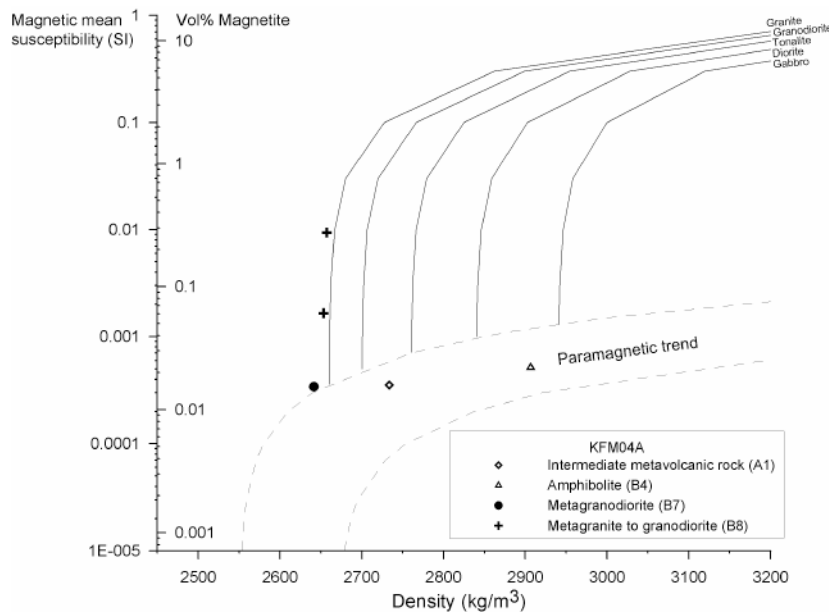


Figure 5-1. Density-susceptibility rock classification diagram for the rocks of KFM04A. See the text for explanation.

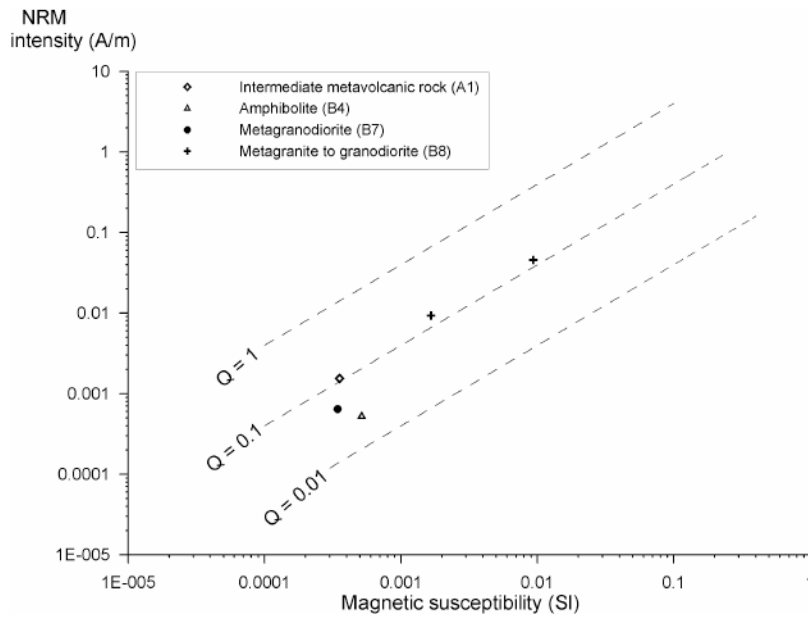


Figure 5-2. NRM intensity versus magnetic susceptibility for the rock samples of KFM04A. Hatched lines indicate Q -values of 0.01, 0.1 and 1. See the text for explanation.

5.1.2 KFM05A

The three metagranite to granodiorite rock samples cluster close to the granite rock classification curve. Their average density is $2,652 \pm 4 \text{ kg/m}^3$ and their average susceptibility is $0.008 \pm 0.004 \text{ SI}$, which are typical values for this rock group /8/. The group C metagranitoid plots close to the granodiorite classification curve and the amphibolite rock sample shows the same characteristics as the corresponding sample from KFM04A with high density and low magnetic susceptibility.

The four group B samples have fairly low Q -values ($Q = 0.02\text{--}0.25$) and the group C metagranitoid has a slightly higher Q -value of $Q = 0.75$, which is unusually high for a group C metagranitoid (Figure 5-4).

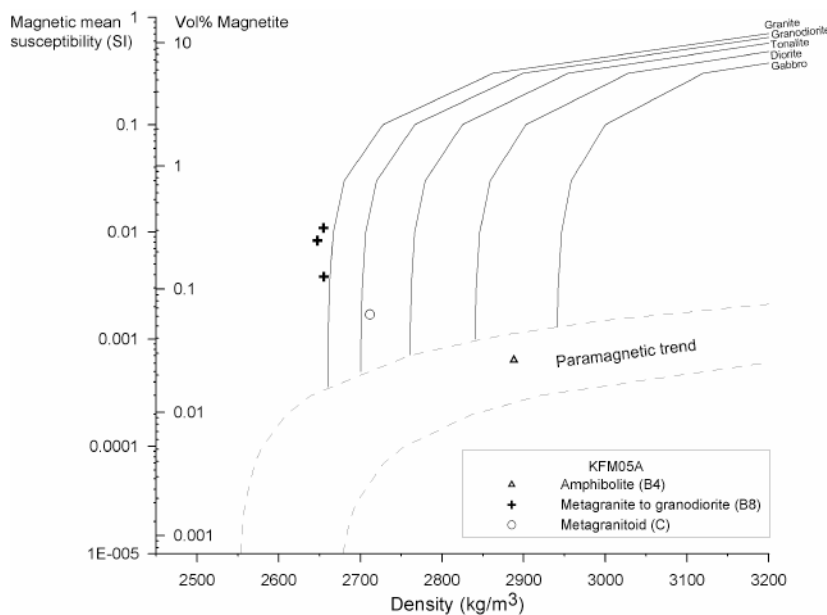


Figure 5-3. Density-susceptibility rock classification diagram for the rocks of KFM05A. See the text for explanation.

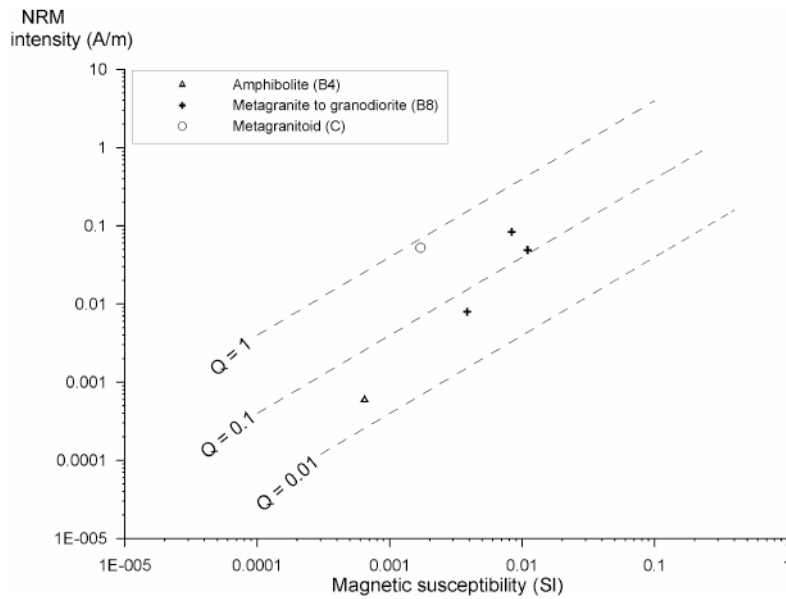


Figure 5-4. NRM intensity versus magnetic susceptibility for the rock samples of KFM05A. Hatched lines indicate Q -values of 0.01, 0.1 and 1. See the text for explanation.

5.1.3 KFM06A

All five measured samples plot on or close to the granite classification curve in Figure 5-5, though the scatter in magnetic susceptibility is high. The average density of the four aplitic granite samples is $2,649 \pm 5 \text{ kg/m}^3$. This is slightly higher than the average density for this rock group, which is $2,635 \pm 9 \text{ kg/m}^3$.

The average Q -value of the aplitic granite samples is $Q = 0.1$, which is normal for this rock type. However, the single metagranite to granodiorite sample has an anomalously high Q -value of $Q = 12.5$. The reason for the high Q -value is the high remanent magnetization intensity of $I_{\text{NRM}} = 451 \text{ mA/m}$ in combination with a rather low magnetic susceptibility. The result indicates that the magnetic mineralogy of this rock samples deviates from what is normal for the metagranite to granodiorite rock type group.

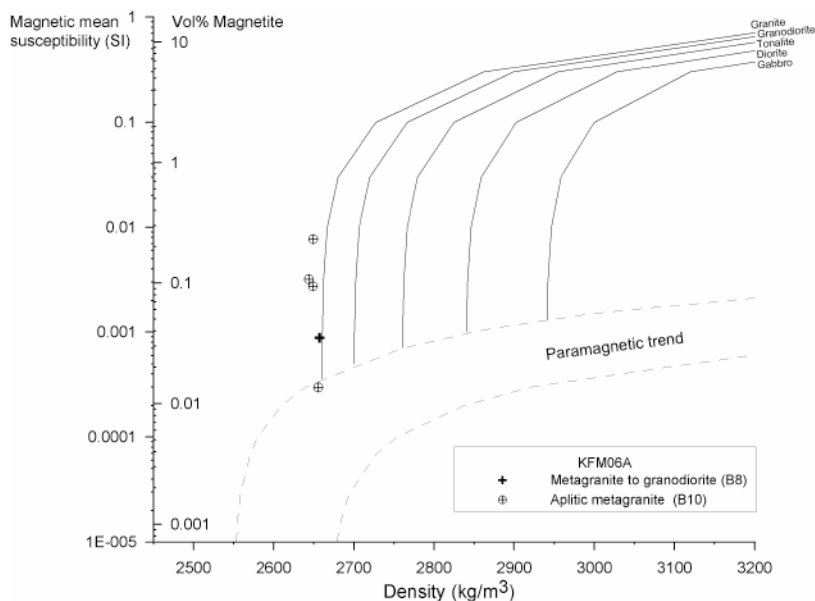


Figure 5-5. Density-susceptibility rock classification diagram for the rocks of KFM06A. See the text for explanation.

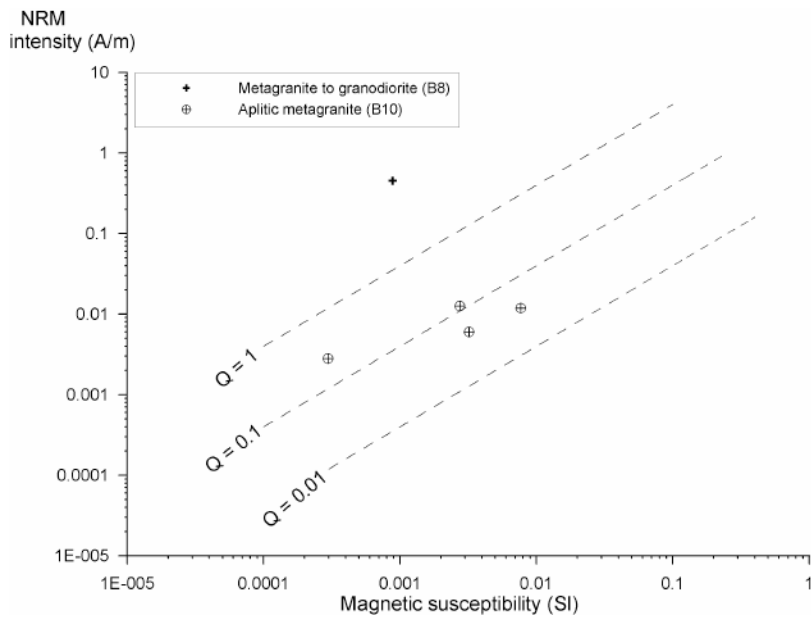


Figure 5-6. NRM intensity versus magnetic susceptibility for the rock samples of KFM06A. Hatched lines indicate Q -values of 0.01, 0.1 and 1. See the text for explanation.

5.2 Anisotropy of magnetic susceptibility (AMS)

The shallow inclination of the three investigated boreholes and the lack of orientation of the rock samples make the interpretations of the orientations of the anisotropy axes meaningless. Thus, in the following chapters presenting the results of the AMS measurements, the diagrams only display shape parameters of the anisotropy ellipsoids.

5.2.1 KFM04A

All five samples from KFM04A have oblate (flattened) ellipsoid shapes, which most likely indicate a dominant compressive deformation and simple shear of the rocks (Figure 5-7). Both metagranite to granodiorite samples have high degree of anisotropy, with a maximum values of $P = 2.06$ of the sample at c 271.5 m section length. Such high degree of anisotropy is an indication that the rock has suffered from a high degree of deformation.

5.2.2 KFM05A

The rock samples in KFM05A show low or moderate degrees of anisotropy and poorly developed ellipsoid shapes (Figure 5-8). The amphibolite sample has a slightly oblate (flattened) ellipsoid shape and two of the metagranite to granodiorite samples show slightly prolate (elongated) ellipsoid shapes. The AMS data indicate low degree of deformation and variations in the type of deformation of the sampled rocks of KFM05A (compare with KFM04A).

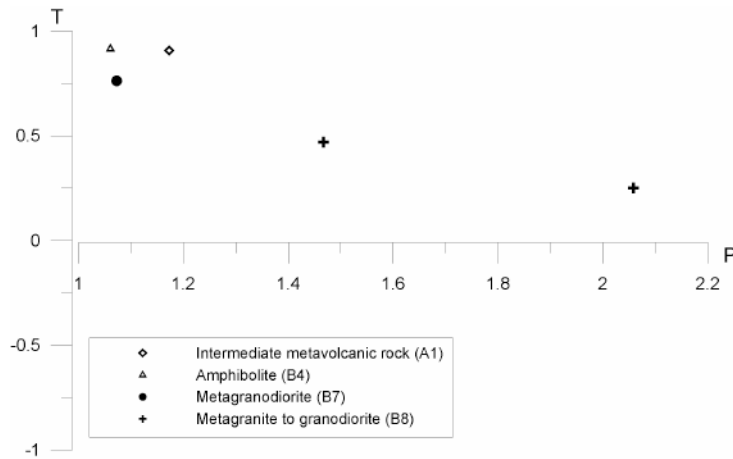


Figure 5-7. Ellipsoid shape (T) plotted versus degree of anisotropy (P) for KFM04A.

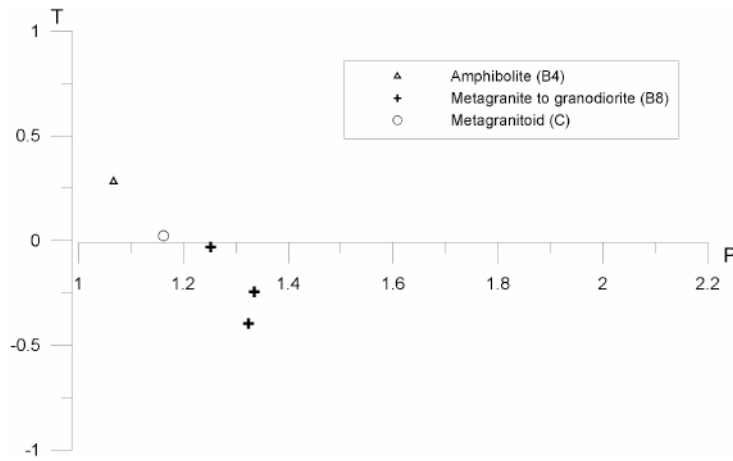


Figure 5-8. Ellipsoid shape (T) plotted versus degree of anisotropy (P) for KFM05A.

5.2.3 KFM06A

All five samples from KFM06A have prolate (elongated) ellipsoid shapes, which most likely indicate a type of deformation related to stretching of the rocks (Figure 5-9). The degree of anisotropy is fairly low for the four aplitic metagranite rock samples and it is high for the metagranite to granodiorite sample. Since no correlation is found between the degree of anisotropy and the volume susceptibility, the data indicate that the metagranite to granodiorite sample has suffered from a higher degree of deformation compared to the aplitic granite, which based on the AMS data appears to be only slightly deformed. Note the differences in ellipsoid shapes (indirectly differences in the type of deformation) between KFM04A and KFM06A

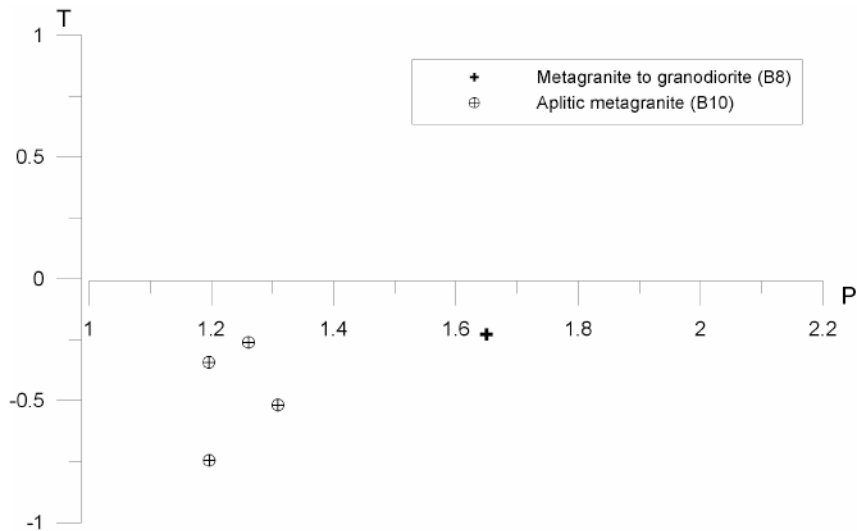


Figure 5-9. Ellipsoid shape (T) plotted versus degree of anisotropy (P) for KFM06A.

5.3 Electrical properties and porosity

5.3.1 KFM04A

The results of the porosity, resistivity and induced polarization (IP) measurements on samples from KFM04A can be seen in Figure 5-10. All samples show fairly normal porosity values of around 0.2 to 0.4%. The amphibolite sample from 737.75 m depth contains sulphides. The resistivity of this sample is considerably lower than for the other samples. This sample also shows high IP values in both fresh and saline water. This indicates that the IP for this sample is mainly due to sulphides and only to a minor part due to membrane polarization.

The other samples show fairly low values of apparent m in Archie's law but high values for apparent a . This is common for ductile deformed and/or altered rock and is indicative of presence of e.g. chlorite, sericite or other fine-grained phyllo-silicates. The resistivity of the samples is thus mainly dependent on the amount of such minerals and only to a lesser extent on the porosity.

Except for the sulphide-bearing sample, the IP values are low and close to zero in saline water. The latter fact indicates that the IP in fresh water is due to membrane polarization for these samples.

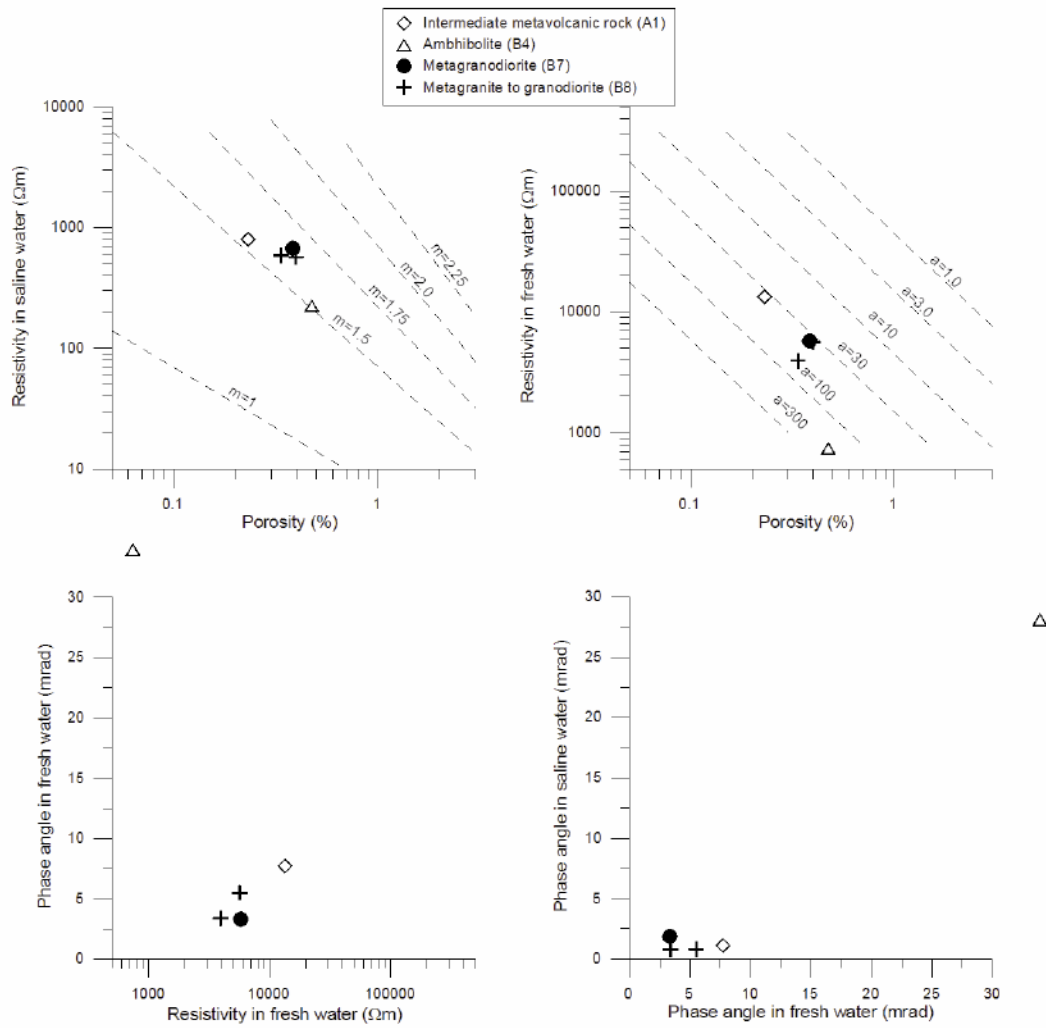


Figure 5-10. Results for KFM04A samples. Top left: Resistivity in saline water (2.5% NaCl by weight) vs porosity, dashed lines show values for Archie's law and $a=4$. Top right: Resistivity in fresh water vs porosity, dashed lines show values for Archie's law and $m=1.6$. Bottom left: IP as phase angle at 0.1 Hz vs resistivity in fresh water. Bottom right: IP in saline water vs IP in fresh water (phase angle at 0.1 Hz).

5.3.2 KFM05A

The results of the porosity, resistivity and IP measurements on samples from KFM05A can be seen in Figure 5-11. All samples show fairly normal porosity values of around 0.2 to 0.4%. The resistivity values are also quite normal in both fresh and saline water.

All samples show fairly low values of apparent m in Archie's law and, except for an amphibolite sample, moderate values for apparent a . The apparent a -values are significantly lower than for the KFM04A samples.

The IP values are low and close to zero in saline water for all KFM05A samples. The latter fact indicates that the IP in fresh water is due to membrane polarization.

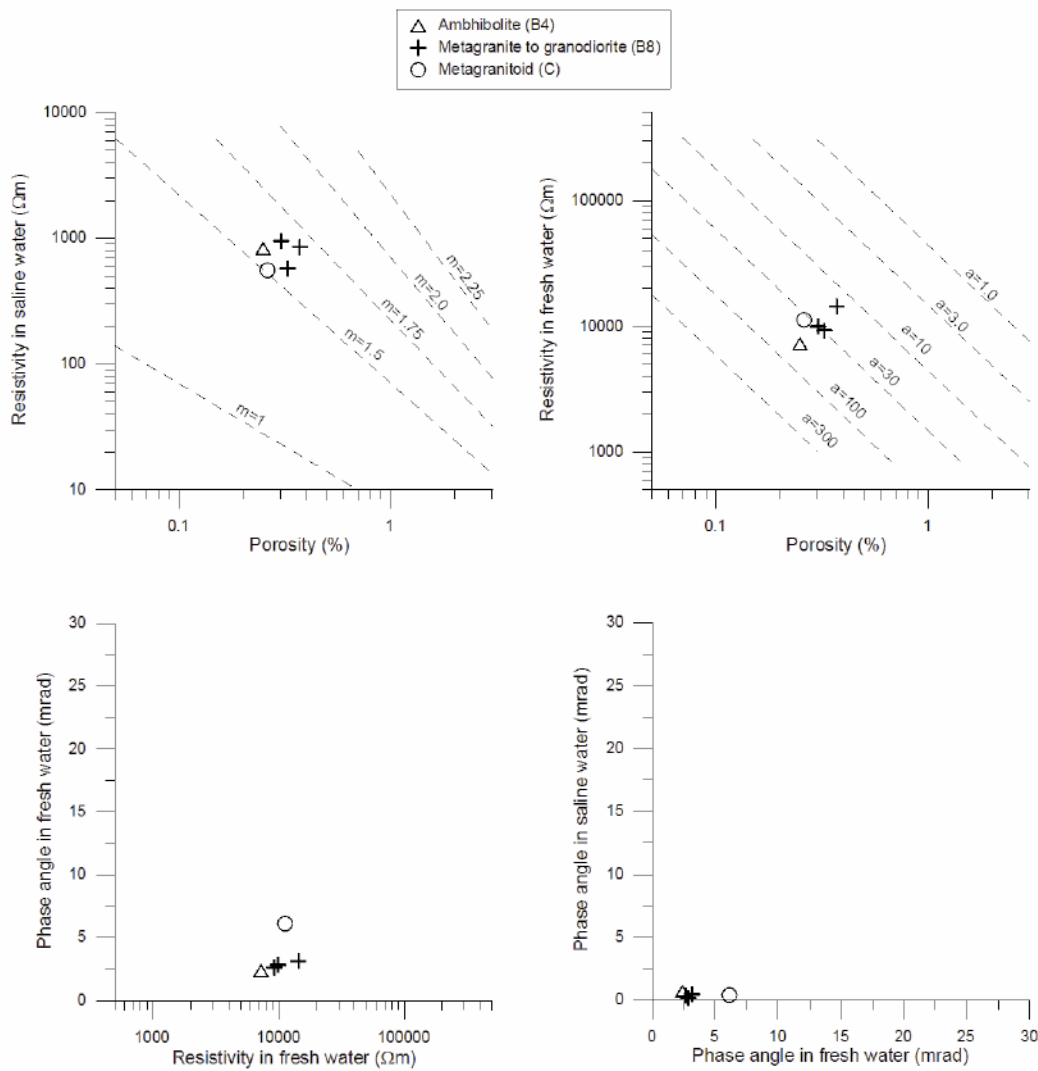


Figure 5-11. Results for KFM05A samples. Top left: Resistivity in saline water (2.5% NaCl by weight) vs porosity, dashed lines show values for Archie's law and $a=4$. Top right: Resistivity in fresh water vs porosity, dashed lines show values for Archie's law and $m=1.6$. Bottom left: IP as phase angle at 0.1 Hz vs resistivity in fresh water. Bottom right: IP in saline water vs IP in fresh water (phase angle at 0.1 Hz).

5.3.3 KFM06A

The results of the porosity, resistivity and IP measurements on samples from KFM06A can be seen in Figure 5-12. All samples show fairly normal porosity values of around 0.2 to 0.4%. The resistivity values are quite normal in fresh water but slightly elevated in fresh water.

All samples show fairly low values of apparent m in Archie's law and, compared to the other two holes, low values for apparent a . Low apparent a -values are expected for aplitic rocks and this results in high resistivities.

The IP values are low in fresh water and close to zero in saline water for all KFM06A samples. The latter fact indicates that the IP in fresh water is due to membrane polarization.

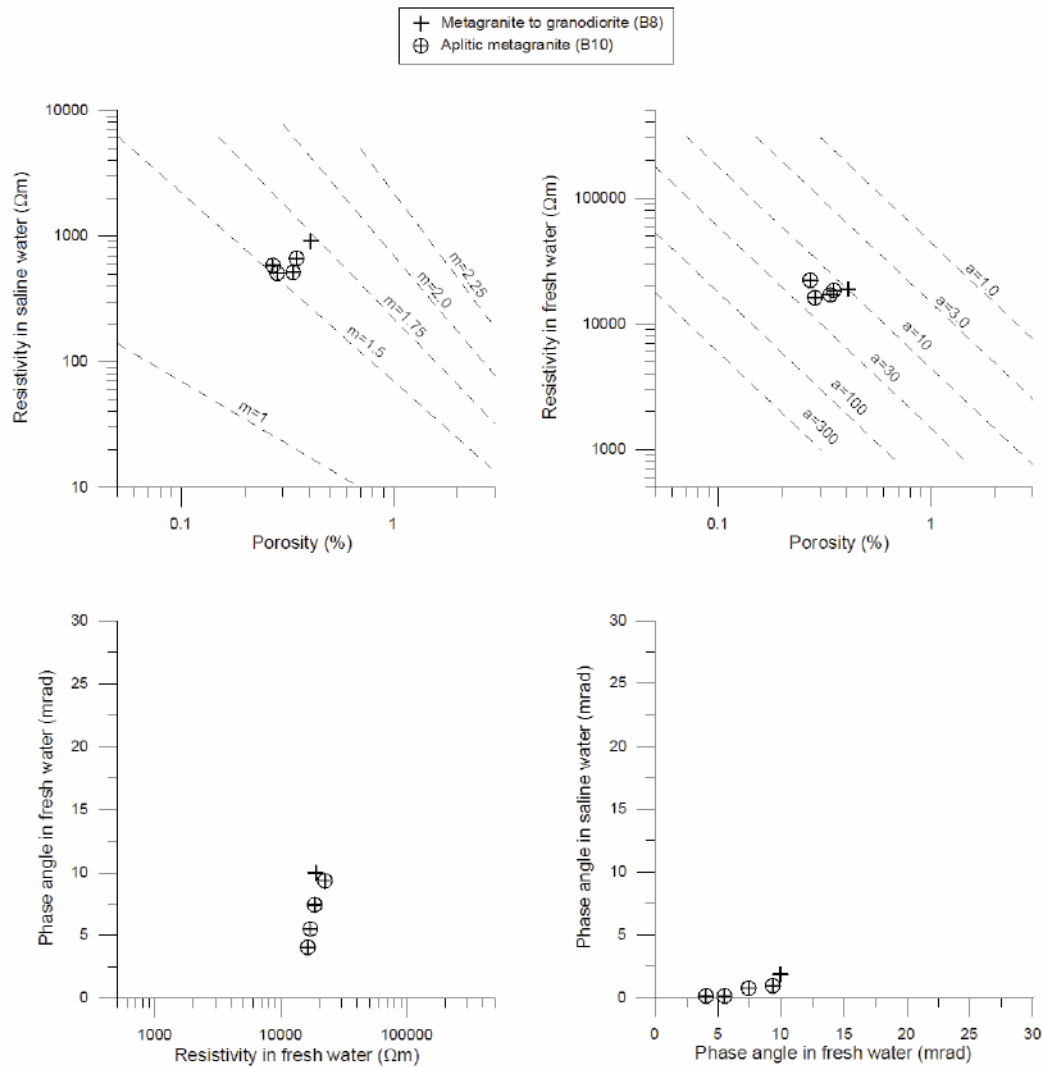


Figure 5-12. Results for KFM06A samples. Top left: Resistivity in saline water (2.5% NaCl by weight) vs porosity, dashed lines show values for Archie's law and $a=4$. Top right: Resistivity in fresh water vs porosity, dashed lines show values for Archie's law and $m=1.6$. Bottom left: IP as phase angle at 0.1 Hz vs resistivity in fresh water. Bottom right: IP in saline water vs IP in fresh water (phase angle at 0.1 Hz).

5.4 Gamma ray spectrometry

The results of the gamma-ray spectrometry laboratory measurements and data processing are presented in Appendix 1.

5.4.1 KFM04A

Results from KFM04A are presented in Figure 5-13, 5-16a and Table 6-1b.

The intermediate metavolcanite (A1) sample at 124.7 m shows normal gamma ray spectrometry characteristics, with potassium, uranium and thorium contents similar to the adjacent (116.6 m) metagranodiorite (B7), 1.7–2.0%, 4–5 ppm and 5–10 ppm respectively.

The amphibolite rock (B4) shows low potassium and uranium content, common for this rock type, that is, a, c 1% potassium and 2 ppm uranium. The thorium content, 7 ppm, is slightly higher than normal.

The potassium and uranium content in the metagranite-granodiorite (B8) is within normal levels for granite, 3.2–3.5% and 5 ppm respectively. The thorium level, 19 ppm, is slightly higher than normal for one sample at 272.7m.

5.4.2 KFM05A

Results from KFM05A are presented in Figure 5-14, 5-16b and Table 6-2b.

The amphibolite rock (B4) shows low potassium, uranium and thorium content, common for this rock type, that is, c 0.8% potassium, 1 ppm uranium and 2 ppm thorium.

The metagranite-granodiorite (B8) is within normal levels for potassium, 2.9–3.4%. The uranium content is slightly lower than normal, 2–4 ppm, while the thorium content is slightly higher than normal 17–20 ppm.

The metagranitoid, group C, sample at 691.6 m shows low potassium, uranium and thorium contents, 1.6%, 2 ppm and 8 ppm respectively, typical for a tonalitic composition.

5.4.3 KFM06A

Results from KFM06A are presented in Figure 5-15, 5-16c and Table 6-3b.

All five samples show a natural exposure rate within normal levels, 10–12 $\mu\text{R/h}$.

The potassium content divides the aplitic metagranite (B10) into two populations. One sample at 636.2 m shows normal values, 3.8% potassium, 3 ppm uranium and 15 ppm thorium. In three samples at deeper levels 818–938 m the potassium content decreases significantly to 0.2–0.6%. The uranium content varies between 2–9 ppm and two of the samples show an increase in thorium, 20–25 ppm.

The metagranite-granodiorite (B8) sample at 757 m shows the same potassium depletion (0.4% K) as the aplitic metagranite. The uranium content is within normal levels, 7 ppm, and thorium shows a slight increase, 19 ppm.

The significant decrease in potassium content for both metagranite-granodiorite (B8) and the aplitic metagranite (B10) indicates a potassium alteration in the deeper sections of the drillhole. The significant potassium depletion is also reflected in the hue-saturation plot, Figure 5-16c.

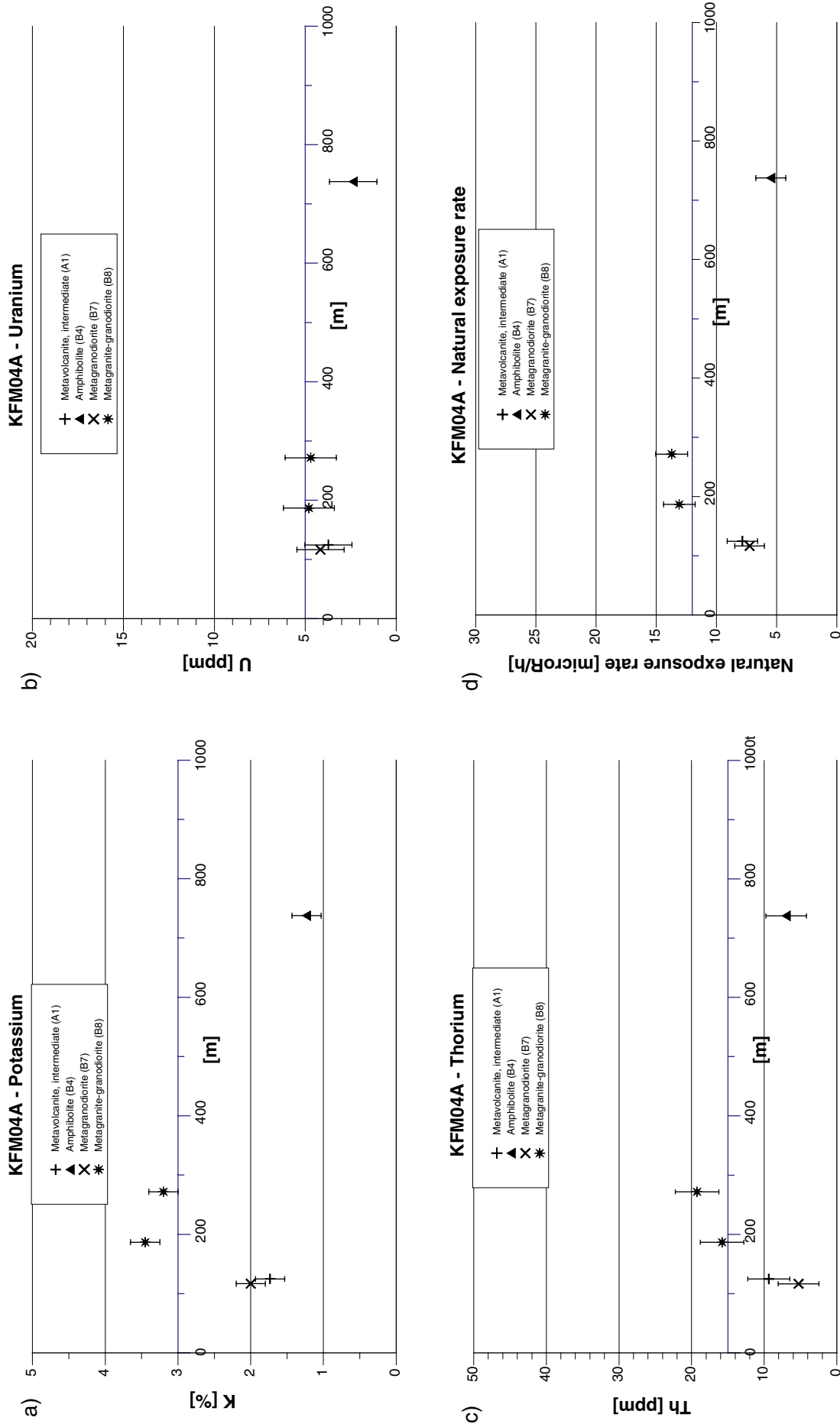


Figure 5-13. Gamma ray spectrometry data for different rock types, plotted with reference to the borehole depth of KFM04A. a) K content, % b) U content, ppm. c) Th content, ppm. d) Natural exposure rate, $\mu\text{R}/\text{h}$. Standard error bars are shown. The borehole axis position represents levels for normal granite.

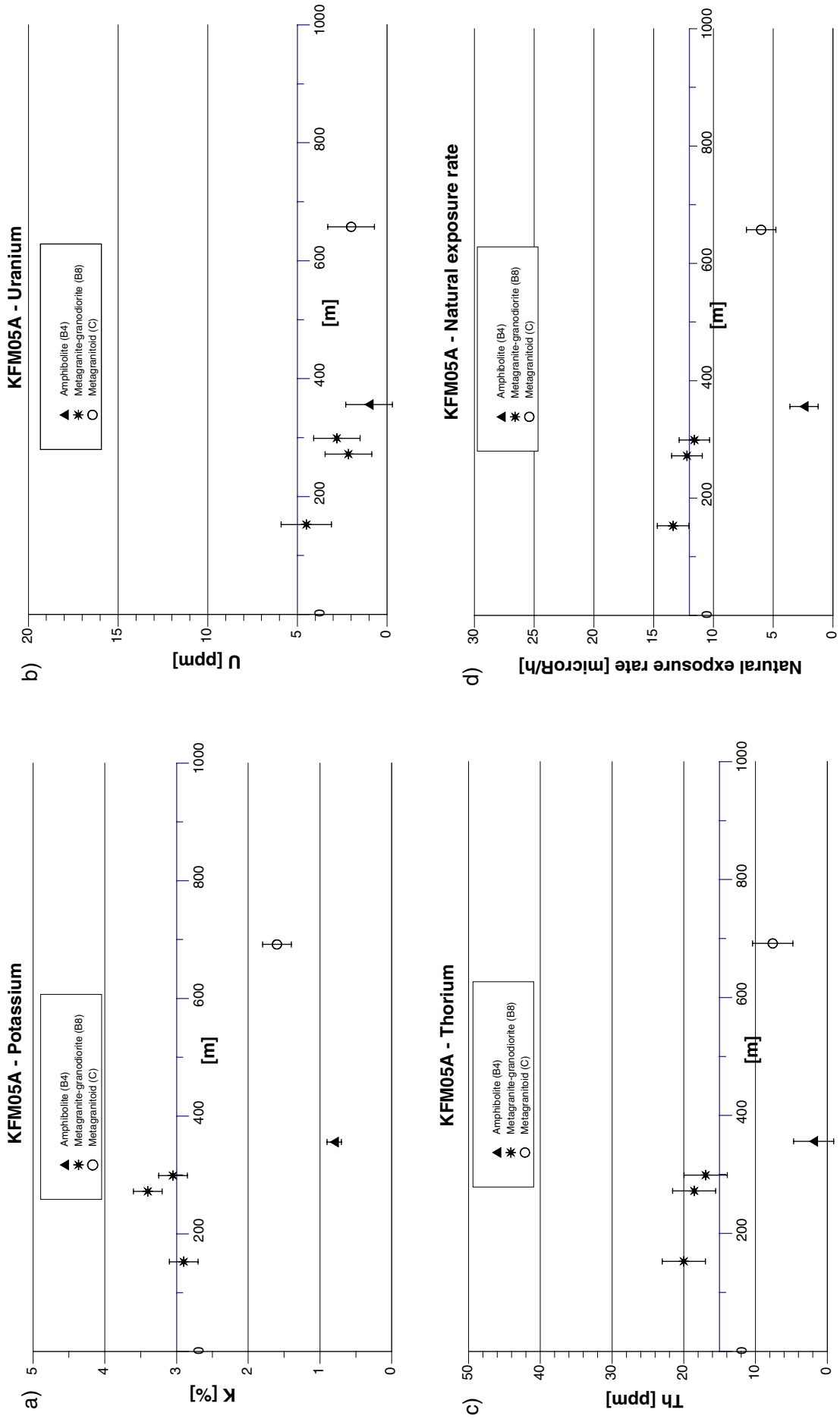


Figure 5-14. Gamma ray spectrometry data for different rock types, plotted with reference to the borehole depth of KFM05A. a) K content, %. b) U content ppm. c) Th content, ppm. d) Natural exposure rate, $\mu\text{R/h}$. Standard error bars are shown. The borehole axis position represents levels for normal granite.

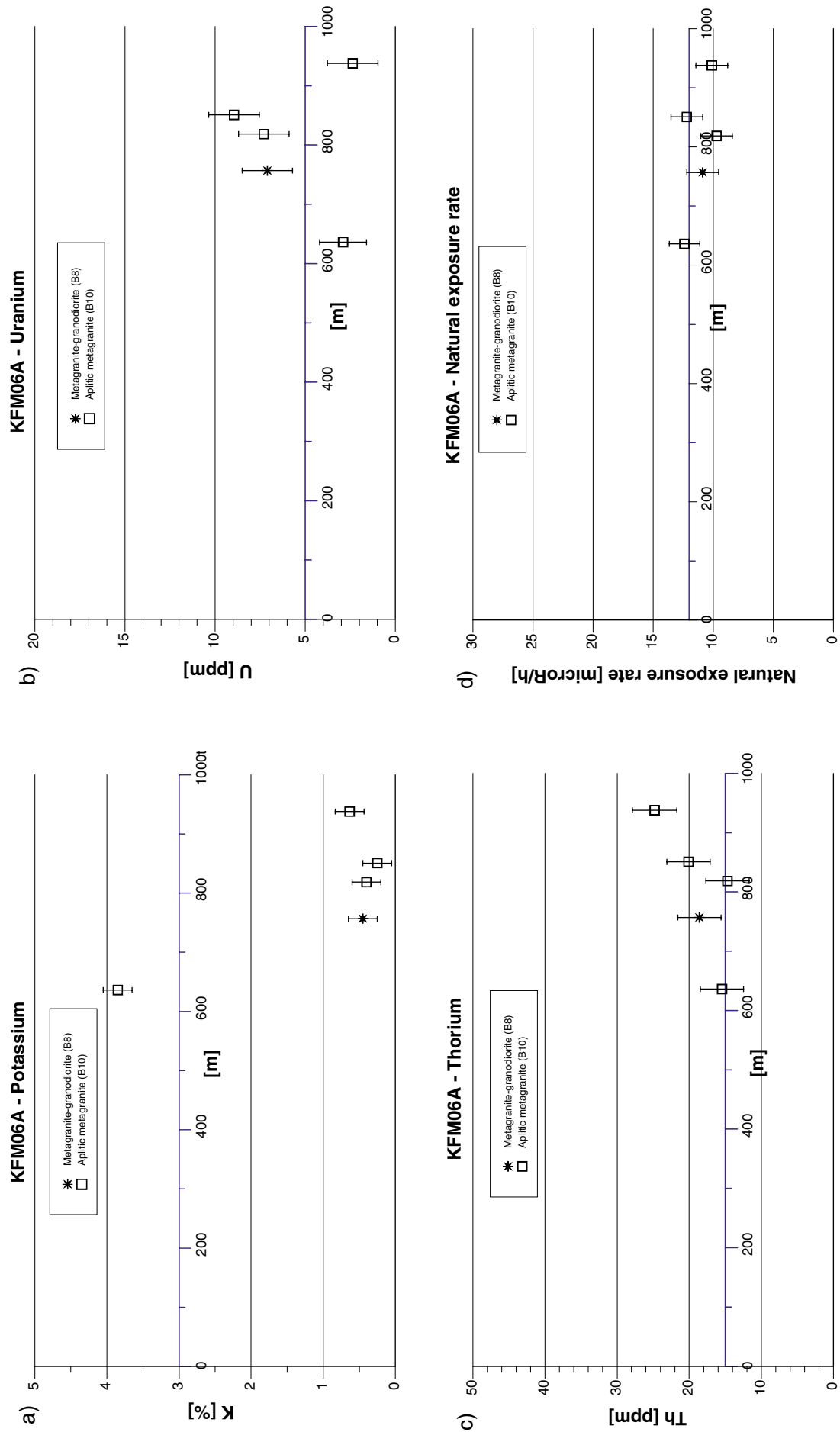


Figure 5-15. Gamma ray spectrometry data for different rock types, plotted with reference to the borehole depth of KFM06A. a) K content, % b) U content, ppm. c) Th content, ppm. d) Natural exposure rate, $\mu\text{R/h}$. Standard error bars are shown. The borehole axis position represents levels for normal granite.

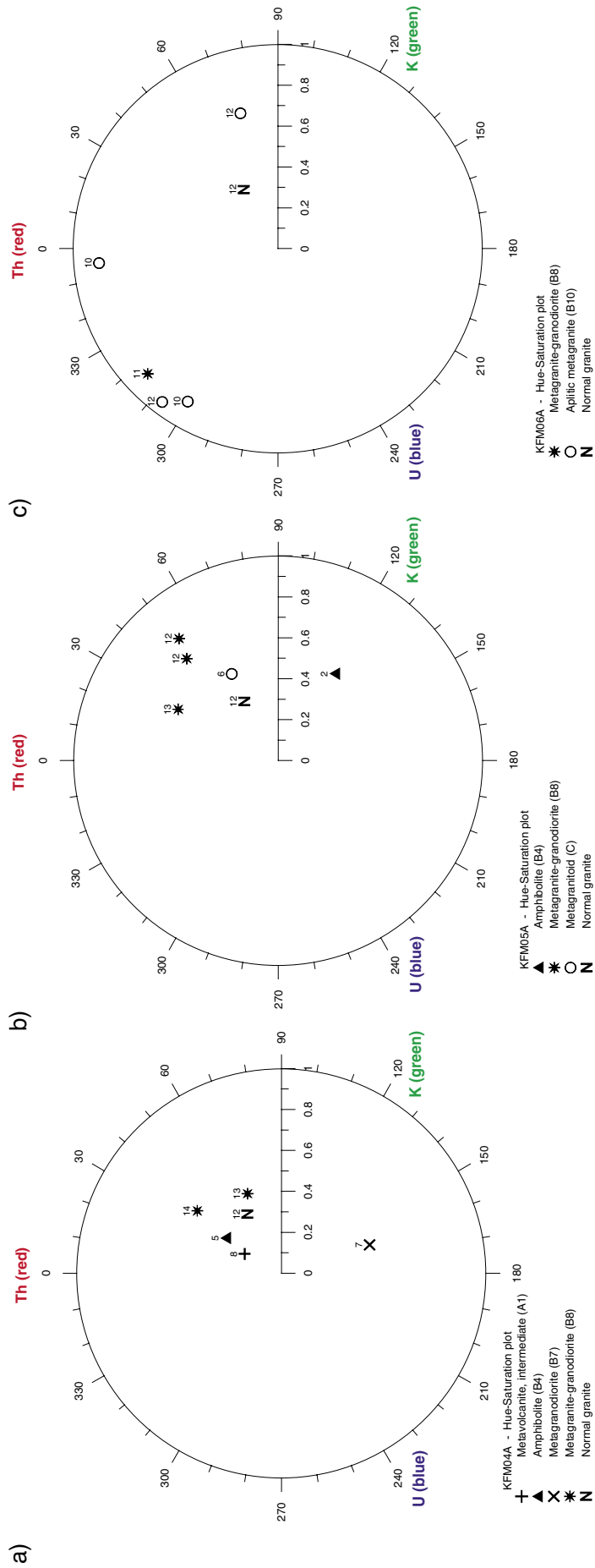


Figure 5-16. Hue-Saturation plot of gamma ray spectrometry measurements on samples from drillhole KFM04A, KFM05A and KFM06A. The presentation shows, for different rock types, the relative distribution between potassium, uranium and thorium in uranium equivalent units (Ur). The letter N marks the position for a normal granite distribution (that is, 3% K, 5 ppm U, 15 ppm Th). Digits show the natural exposure in $\mu\text{R/h}$. a) KFM04A b) KFM05A c) KFM06A

6 Compilation of petrophysical parameters

The tables below present a compilation of some petrophysical parameters and gamma-ray spectrometry data for each borehole respectively, KFM04A (Table 6-1a,b), KFM05A (Table 6-2a,b) and KFM06A (Table 6-3a,b).

Table 6-1a. Some petrophysical parameters of KFM04A.

sec up (m)	sec low (m)	wet density (kg/m ³)	porosity (%)	Kmean (SI)	Remanence intensity (A/m)	Q value (SI)	Resistivity (Ωm) fresh water	IP at 0.1 Hz (mrad) fresh water	Rock group	Results of the petrophysical rock classification (Figure 5-1)
116.86	117.06	2,641	0.38	0.000344	0.00064	0.05	5,763	3.3	B7	Granite
124.80	125.00	2,733	0.23	0.000354	0.00154	0.11	13,367	7.7	A1	Rhyo-dacite
186.80	187.00	2,653	0.40	0.001659	0.00935	0.14	5,639	5.5	B8	Granite
271.44	271.64	2,657	0.34	0.009330	0.04577	0.12	3,949	3.4	B8	Granite
737.65	737.85	2,907	0.47	0.000515	0.00052	0.02	742	33.9	B4	Mafic volcanite

Table 6-1b. Gamma-ray spectrometry data from KFM04A.

Sec up (m)	Sec low (m)	K [%]	U [ppm]	Th [ppm]	Natural exposure [micro-R/h]	Rock group	Rock type	Rock code
116.51	116.7	2.00	4.17	5.27	7.2	B7	Metagranodiorite	101056
124.6	124.8	1.73	3.73	9.37	7.8	A1	Metavolcanite. intermediate	103076
186.57	186.8	3.45	4.80	15.80	13.1	B8/B9	Metagranite-granodiorite	101057
271.64	271.84	3.20	4.70	19.25	13.7	B8/B9	Metagranite-granodiorite	101057
737.41	737.61	1.23	2.37	6.97	5.5	B4	Amphibolite	102017

Table 6-2a. Some petrophysical parameters of KFM05A.

sec up (m)	sec low (m)	wet density (kg/m ³)	porosity (%)	Kmean (SI)	Remanence intensity (A/m)	Q value (SI)	Resistivity (Ωm) fresh water	IP at 0.1 Hz (mrad) fresh water	Rock group	Results of the petrophysical rock classification (Figure 5-3)
152.26	152.46	2,655	0.30	0.010950	0.04874	0.11	9,898	2.9	B8	Granite
272.45	272.65	2,647	0.37	0.008295	0.08380	0.25	14,337	3.2	B8	Granite
298.62	298.82	2,655	0.33	0.003825	0.00794	0.05	9,280	2.6	B8	Granite
356.50	356.70	2,888	0.25	0.000642	0.00059	0.02	7,234	2.4	B4	Mafic volcanite
691.38	691.58	2,712	0.26	0.001705	0.05214	0.75	11,222	6.1	C	Granodiorite

Table 6-2b. Gamma-ray spectrometry data from KFM05A.

Sec up (m)	Sec low (m)	K [%]	U [ppm]	Th [ppm]	Natural exposure [micro-R/h]	Rock group	Rock type	Rock code
152.46	152.66	2.90	4.50	20.00	13.4	B8/B9	Metagranite-granodiorite	101057
271.9	272.11	3.40	2.15	18.55	12.2	B8/B9	Metagranite-granodiorite	101057
298.82	299.02	3.05	2.80	16.95	11.6	B8/B9	Metagranite-granodiorite	101057
355.87	356.07	0.80	1.00	1.90	2.4	B4	Amphibolite	102017
691.58	691.78	1.60	2.00	7.60	6.0	C	Metagranitoid	101051

Table 6-3a. Some petrophysical parameters of KFM06A.

sec up (m)	sec low (m)	wet density (kg/m ³)	porosity (%)	Kmean (SI)	Remanence intensity (A/m)	Q value (SI)	Resistivity (Ω m) fresh water	IP at 0.1 Hz (mrad) fresh water	Rock group	Results of the petrophysical rock classification (Figure 5-5)
635.80	636.00	2.649	0.35	0.002744	0.01263	0.11	18.424	7.4	B10	Granite
757.02	757.22	2.657	0.41	0.000882	0.45120	12.48	18.971	10.0	B8	Granite
817.86	818.06	2.656	0.27	0.000297	0.00280	0.23	22.247	9.3	B10	Granite
851.13	851.33	2.649	0.28	0.007690	0.01190	0.04	16.226	4.0	B10	Granite
939.04	939.24	2.644	0.34	0.003206	0.00599	0.05	17.022	5.5	B10	Granite

Table 6-3b. Gamma-ray spectrometry data from KFM06A.

Sec up (m)	Sec low (m)	K [%]	U [ppm]	Th [ppm]	Natural exposure [micro-R/h]	Rock group	Rock type	Rock code
636.14	636.34	3.85	2.90	15.45	12.4	B10	Aplitic metagranite	101058
756.82	757.02	0.45	7.10	18.60	10.9	B8/B9	Metagranite-granodiorite	101057
818.42	818.62	0.40	7.30	14.70	9.7	B10	Aplitic metagranite	101058
850.59	850.79	0.25	8.95	20.10	12.2	B10	Aplitic metagranite	101058
937.75	937.95	0.63	2.37	24.80	10.1	B10	Aplitic metagranite	101058

6.1 Comments on the results

There is a general agreement between the geological rock classification and the geophysical rock classification indicated by the density-susceptibility diagrams. A significant deviation from this is the metagranodiorite (B7) sample from KFM04A, which plots as a low density granite (Figure 5-1). A very high Q-value of $Q = 12.5$ is reported for a metagranite to granodiorite sample in KFM06A. The result indicates that the magnetic mineralogy of the rock sample deviates from what is normal for this rock type group. Apart from this deviation, the Q-values are moderate or low.

The AMS data indicate that the rocks in the vicinities of the three investigated boreholes have suffered from different types of deformation. The samples of KFM04A have flattened ellipsoids and partly strong degree of anisotropy, which indicates strong compressive deformation. In KFM05A the AMS fabric is poorly developed, which is characteristic for a low degree of deformation. The rock samples in KFM06A show elongated AMS ellipsoids, which probably indicate a dominant stretching type of deformation.

All investigated rock samples show fairly normal porosity values for crystalline rocks. The KFM04A samples have electrical properties indicative of strong surface conductivity that probably is related to presence of fine-grained phyllo-silicates like e.g. chlorite. One sample from KFM04A containing sulphides has low resistivity and high IP effect.

The sampled rock types in general show a normal distribution of potassium, uranium and thorium. However, in the deeper part of KFM06A both aplitic metagranite and metagranite-granodiorite show a strong depletion in potassium, with a content of 0.2–0.6% K.

References

- /1/ **Mattsson H, Isaksson H, Thunehed H, 2003.** Petrophysical rock sampling, measurements of petrophysical rock parameters and in situ gamma ray spectrometry measurements on outcrops carried out 2002. SKB P-03-26, Svensk Kärnbränslehantering AB.
- /2/ **Pettersson J, Tullborg E-L, Berglund J, Lindroos H, Danielsson P, Wängnerud A, Mattsson H, Thunehed H, Isaksson H.** Petrography, geochemistry, petrophysics and fracture mineralogy of boreholes KFM01A, KFM02A and KFM03A+B. SKB P-04-103, Svensk Kärnbränslehantering AB.
- /3/ **Pettersson J, Berglund J, Danielsson P, Skogsmo G, 2005.** Petrographic and geochemical characteristics of bedrock samples from boreholes KFM04A-06A, and a whitened alteration rock. Forsmark site investigation. SKB P-05-156. Svensk Kärnbränslehantering AB.
- /4/ **Henkel H, 1991.** Petrophysical properties (density and magnetization of rocks from the northern part of the Baltic Shield). *Tectonophysics* 192, page1–19.
- /5/ **Collinson D W, 1983.** *Methods in rock magnetism and paleomagnetism*, Chapman and Hall, London, United Kingdom. 503 pp.
- /6/ **Parasnis D S, 1997.** *Principles of applied geophysics*. Chapman and Hall, London, 429 pp.
- /7/ **Puranen R, 1989.** Susceptibilities, iron and magnetite content of Precambrian rocks in Finland. Geological survey of Finland, Report of investigations 90, 45 pp.
- /8/ **Isaksson H, Mattsson H, Thunehed H, Keisu M, 2002.** Interpretation of petrophysical surface data Stage 1. SKB P-03-102, Svensk Kärnbränslehantering AB.
- /9/ **Tarling D H, Hrouda F, 1993.** *The magnetic anisotropy of rocks*, Chapman and Hall, London, United Kingdom. 217 pp.
- /10/ **Archie G E, 1942.** The electrical resistivity log as an aid in determining some reservoir characteristics: *Trans. Am. Inst. Min. Metallurg. Petr.Eng.* 146, 54–62.
- /11/ **Keller G V, Frischknecht F C, 1966.** *Electrical methods in geophysical prospecting*. Pergamon Press.
- /12/ **Grasty R L, Carson J M, Charbonneau B W, Holman P B, 1984.** Natural Background Radiation in Canada; Geological Survey of Canada, Bulletin 360, 39 p.

Appendix 1

Drillhole- ID	Sec up (m)	Sec low (m)	SGU ID	No of mea- sure- ments	K mean [%]	K max [%]	K min [%]	Diff. from mean [%]	U mean [ppm]	U max [ppm]	U min [ppm]	Diff. from mean [%]	Th mean [ppm]	Th max [ppm]	Th min [ppm]	Diff. from mean [%]	K mean error	U mean error	Th mean error	Gamma index	Natural expo- sure [µR/h]
KFM04A	116.51	116.70	SKB050001	3	2.0	2.1	1.8	10.0	4.2	4.3	3.9	6.4	5.3	5.9	4.1	22.2	0.2	1.3	2.8	0.49	7.2
KFM04A	124.60	124.80	SKB050002	3	1.7	1.8	1.6	7.7	3.7	4.9	3.0	31.3	9.4	11.2	8.1	19.6	0.2	1.3	2.9	0.52	7.8
KFM04A	186.57	186.80	SKB050003	2	3.5	3.5	3.4	1.4	4.8	5.4	4.2	12.5	15.8	17.8	13.8	12.7	0.2	1.4	3.0	0.88	13.1
KFM04A	271.64	271.84	SKB050004	2	3.2	3.2	3.2	0.0	4.7	4.9	4.5	4.3	19.3	21.2	17.3	10.1	0.2	1.4	3.1	0.92	13.7
KFM04A	737.41	737.61	SKB050005	3	1.2	1.3	1.2	5.4	2.4	3.9	0.5	78.9	7.0	11.6	2.5	66.5	0.2	1.3	2.8	0.37	5.5
KFM05A	152.46	152.66	SKB050006	2	2.9	3.1	2.7	6.9	4.5	5.1	3.9	13.3	20.0	22.1	17.9	10.5	0.2	1.4	3.1	0.89	13.4
KFM05A	271.90	272.11	SKB050007	2	3.4	3.4	3.4	0.0	2.2	2.3	2.0	7.0	18.6	20.0	17.1	7.8	0.2	1.3	3.1	0.82	12.2
KFM05A	298.82	299.02	SKB050008	2	3.1	3.2	2.9	4.9	2.8	3.6	2.0	28.6	17.0	17.9	16.0	5.6	0.2	1.3	3.0	0.78	11.6
KFM05A	355.87	356.07	SKB050009	2	0.8	0.9	0.7	12.5	1.0	2.0	0.0	100.0	1.9	3.8	0.0	100.0	0.2	1.3	2.8	0.16	2.4
KFM05A	691.58	691.78	SKB050010	2	1.6	2.0	1.2	25.0	2.0	3.6	0.4	80.0	7.6	9.7	5.5	27.6	0.2	1.3	2.9	0.40	6.0
KFM06A	636.14	636.34	SKB050011	2	3.9	3.9	3.8	1.3	2.9	4.2	1.6	44.8	15.5	16.8	14.1	8.7	0.2	1.3	3.0	0.83	12.4
KFM06A	756.82	757.02	SKB050012	2	0.5	0.5	0.4	11.1	7.1	9.2	5.0	29.6	18.6	23.0	14.2	23.7	0.2	1.4	3.1	0.71	10.9
KFM06A	818.42	818.62	SKB050013	2	0.4	0.5	0.3	25.0	7.3	8.6	6.0	17.8	14.7	17.1	12.3	16.3	0.2	1.4	3.0	0.64	9.7
KFM06A	850.59	850.79	SKB050014	2	0.3	0.4	0.1	60.0	9.0	10.3	7.6	15.1	20.1	21.5	18.7	7.0	0.2	1.4	3.1	0.80	12.2
KFM06A	937.75	937.95	SKB050015	3	0.6	0.8	0.5	26.3	2.4	4.2	0.6	77.5	24.8	28.1	23.0	13.3	0.2	1.4	3.1	0.66	10.1